Eur. Phys. J. E **1**, 55–59 (2000)

THE EUROPEAN PHYSICAL JOURNAL E

EDP Sciences

Convection in horizontally shaken granular material

C. Salueña[1,2] and T. Pöschel[2,a]

[1] Departament de Física Fonamental, Divisió de Ciències Experimentals i Matemàtiques, Universitat de Barcelona, Spain
[2] Humboldt-Universität zu Berlin[b], Institut für Physik, Invalidenstraße 110, 10115 Berlin, Germany

Received 3 March 1999

Abstract. In horizontally shaken granular material different types of pattern formation have been reported. We want to deal with the convection instability which has been observed in experiments and which recently has been investigated numerically. Using two dimensional molecular dynamics we show that the convection pattern depends crucially on the inelastic properties of the material. The concept of restitution coefficient provides arguments for the change of the behaviour with varying inelasticity.

PACS. 81.05.Rm Porous materials; granular materials – 83.70.Fn Granular solids – 46.40.-f Vibrations and mechanical waves

1 Introduction

When granular material in a cubic container is shaken horizontally one observes experimentally different types of instabilities, *i.e.* spontaneous formation of ripples in shallow beds [1], liquefaction [2,3], convective motion [4,5] and recurrent swelling of shaken material where the period of swelling decouples from the forcing period [6]. Other interesting experimental results concerning simultaneously vertically and horizontally vibrated granular systems [7] and enhanced packing of spheres due to horizontal vibrations [8] have been reported recently. Horizontally shaken granular systems have been simulated numerically using cellular automata [1] as well as molecular dynamics techniques [2,3,9–12]. Theoretical work on horizontal shaking can be found in [11] and the dynamics of a single particle in a horizontally shaken box has been discussed in [13].

Recently the effect of convection in a horizontally shaken box filled with granular material attracted much attention and presently the effect is studied experimentally by different groups [4–6]. Unlike the effect of convective motion in vertically shaken granular material which has been studied intensively experimentally, analytically and by means of computer simulations (see *e.g.* [14–17]), there exist only a few references on horizontal shaking. Different from the vertical case, where the "architecture" of the convection pattern is very simple [18], in horizontally shaken containers one observes a variety of different patterns, convecting in different directions, in parallel as well as perpendicular to the direction of forcing [4]. Under certain conditions one observes several convection rolls on top of each other [5]. An impression of the complicated convection can be found in the internet [19].

Whereas the properties of convection in vertically shaken systems can be reproduced by two dimensional molecular dynamics simulations with good reliability, for the case of horizontal motion the results of simulations are inconsistent with the experimental results: in *all* experimental investigations it was reported that the material flows downwards close to the vertical walls [4–6,19], but reported numerical simulations systematically show surface rolls in opposite direction accompanying the more realistic deeper rolls, or even replacing them completely [10].

Our investigation is thus concerned with the convection pattern, *i.e.* the number and direction of the convection rolls in a two dimensional molecular dynamics simulation. We will show that the choice of the dissipative material parameters has crucial influence on the convection pattern and, in particular, that the type of convection rolls observed experimentally can be reproduced by using sufficiently high dissipation constants.

2 Numerical model

The system under consideration is sketched in Figure 1: we simulate a two-dimensional vertical cross-section of a three-dimensional container. This rectangular section of width $L = 100$ (all units in cgs system), and infinite height, contains $N = 1000$ spherical particles. The system is periodically driven by an external oscillator $x(t) = A\sin(2\pi ft)$ along a horizontal plane. For the effect we want to show, a working frequency $f = 10$ and amplitude $A = 4$ is selected. These values give an acceleration amplitude of approximately $16g$. Lower accelerations affect the intensity of the convection but do not change the basic features of the convection pattern which we want to discuss. As has been shown in [12],

[a] e-mail: thorsten@physik.hu-berlin.de
[b] http://summa.physik.hu-berlin.de/~kies/

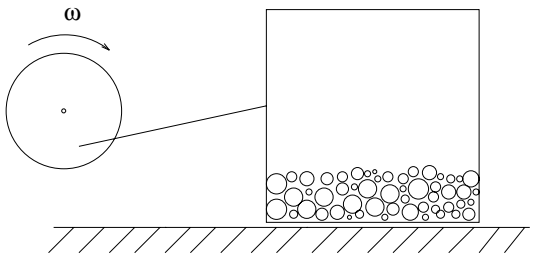

Fig. 1. Sketch of the simulated system.

past the fluidization point, a much better indicator of the convective state is the dimensionless velocity $A2\pi f/\sqrt{Lg}$. This means that in small containers motion saturates earlier, hence, results for different container lengths at the same values of the acceleration amplitude cannot be compared directly. Our acceleration amplitude $\approx 16g$ corresponds to $\approx 3g$ in a 10 cm container (provided that the frequency is the same and particle sizes have been scaled by the same amount).

The radii of the particles of density 2 are homogeneously distributed in the interval $[0.6, 1.4]$. The rough inner walls of the container are simulated by attaching additional particles of the same radii and material properties (this simulation technique is similar to "real" experiments, *e.g.* [15]).

For the molecular dynamics simulations, we apply a modified soft-particle model by Cundall and Strack [20]: Two particles i and j, with radii R_i and R_j and at positions $\mathbf{r}_i$ and $\mathbf{r}_j$, interact if their compression $\xi_{ij} = R_i + R_j - |\mathbf{r}_i - \mathbf{r}_j|$ is positive. In this case the colliding spheres feel the force $F_{ij}^{\mathrm{N}}\mathbf{n}^{\mathrm{N}} + F_{ij}^{\mathrm{S}}\mathbf{n}^{\mathrm{S}}$, with $\mathbf{n}^{\mathrm{N}}$ and $\mathbf{n}^{\mathrm{S}}$ being the unit vectors in normal and shear direction. The normal force acting between colliding spheres reads

$$F_{ij}^{\mathrm{N}} = \frac{Y\sqrt{R_{ij}^{\mathrm{eff}}}}{1-\nu^2}\left(\frac{2}{3}\xi_{ij}^{3/2} + B\sqrt{\xi_{ij}}\frac{\mathrm{d}\xi_{ij}}{\mathrm{d}t}\right) \qquad (1)$$

where Y is the Young modulus, ν is the Poisson ratio and B is a material constant which characterizes the dissipative character of the material [21].

$$R_{ij}^{\mathrm{eff}} = (R_i R_j)\,/\,(R_i + R_j) \qquad (2)$$

is the effective radius. For a strict derivation of (1) see [21,22].

For the shear force we apply the model by Haff and Werner [23]

$$F_{ij}^{\mathrm{S}} = \mathrm{sign}\left(v_{ij}^{\mathrm{rel}}\right)\min\left\{\gamma_{\mathrm{s}} m_{ij}^{\mathrm{eff}}\left|v_{ij}^{\mathrm{rel}}\right|,\, \mu\left|F_{ij}^{\mathrm{N}}\right|\right\} \qquad (3)$$

with the effective mass $m_{ij}^{\mathrm{eff}} = (m_i m_j)\,/\,(m_i + m_j)$ and the relative velocity at the point of contact

$$v_{ij}^{\mathrm{rel}} = (\dot{\mathbf{r}}_i - \dot{\mathbf{r}}_j)\cdot\mathbf{n}^{\mathrm{S}} + R_i\Omega_i + R_j\Omega_j. \qquad (4)$$

Ω_i and Ω_j are the angular velocities of the particles.

The resulting momenta M_i and M_j acting upon the particles are $M_i = F_{ij}^{\mathrm{S}}R_i$ and $M_j = -F_{ij}^{\mathrm{S}}R_j$. Equation (3) takes into account that the particles slide upon each other for the case that the Coulomb condition $\mu|F_{ij}^{\mathrm{N}}| < \left|F_{ij}^{\mathrm{S}}\right|$ holds, otherwise they feel some viscous friction. By means of $\gamma_{\mathrm{n}} \equiv BY/(1-\nu^2)$ and γ_{s}, normal and shear damping coefficients, energy loss during particle contact is taken into account [24].

The equations of motion for translation and rotation have been solved using a Gear predictor-corrector scheme of sixth order (*e.g.* [25]).

The values of the coefficients used in simulations are $Y/(1-\nu^2) = 1\times10^8$, $\gamma_{\mathrm{s}} = 1\times10^3$, $\mu = 0.5$. For the effect we want to show, the coefficient γ_{n} takes values within the range $\left[10^2, 10^4\right]$.

3 Results

The mechanisms for convection under horizontal shaking have been discussed in [10]. Now we can show that these mechanisms can be better understood by taking into account the particular role of dissipation in this problem. The most striking consequence of varying the normal damping coefficient is the change in organization of the convective pattern, *i.e.* the direction and number of rolls in the stationary regime. This is shown in Figure 2, which has been obtained after averaging particle displacements over 200 cycles (2 snapshots per cycle). The asymmetry of compression and expansion of particles close to the walls (where the material results highly compressible) explains the large transverse velocities shown in the figure. Note, however, that the upward and downward motion at the walls cannot be altered by this particular averaging procedure.

The first frame shows a convection pattern with only two rolls, where the arrows indicate that the grains slide down the walls, with at most a slight expansion of the material at the surface. There are no surface rolls. This is very similar to what has been observed in experiments [4–6]. In this case, dissipation is high enough to damp most of the sloshing induced by the vertical walls, and not even the grains just below the surface can overcome the pressure gradient directed downwards.

For lower damping, we see the developing of surface rolls, which coexist with the inner rolls circulating in the opposite way. Some energy is now available for upward motion when the walls compress the material fluidized during the opening of the wall "gap" (empty space which is created alternatively during the shaking motion). This is the case reported in [10]. The last frames demonstrate how the original rolls vanish at the same time that the surface rolls grow occupying a significant part of the system. Another feature shown in the figure is the thin layer of material involving 3 particle rows close to the bottom, which perform a different kind of motion. This effect, which can be seen in all frames, is due to the presence of the constraining boundaries but has not been analyzed separately.

With decreasing normal damping γ_{n} there are two transitions observable in Figure 2, meaning that the convection pattern changes qualitatively at these two particular values of γ_{n}: the first transition leads to the appearance

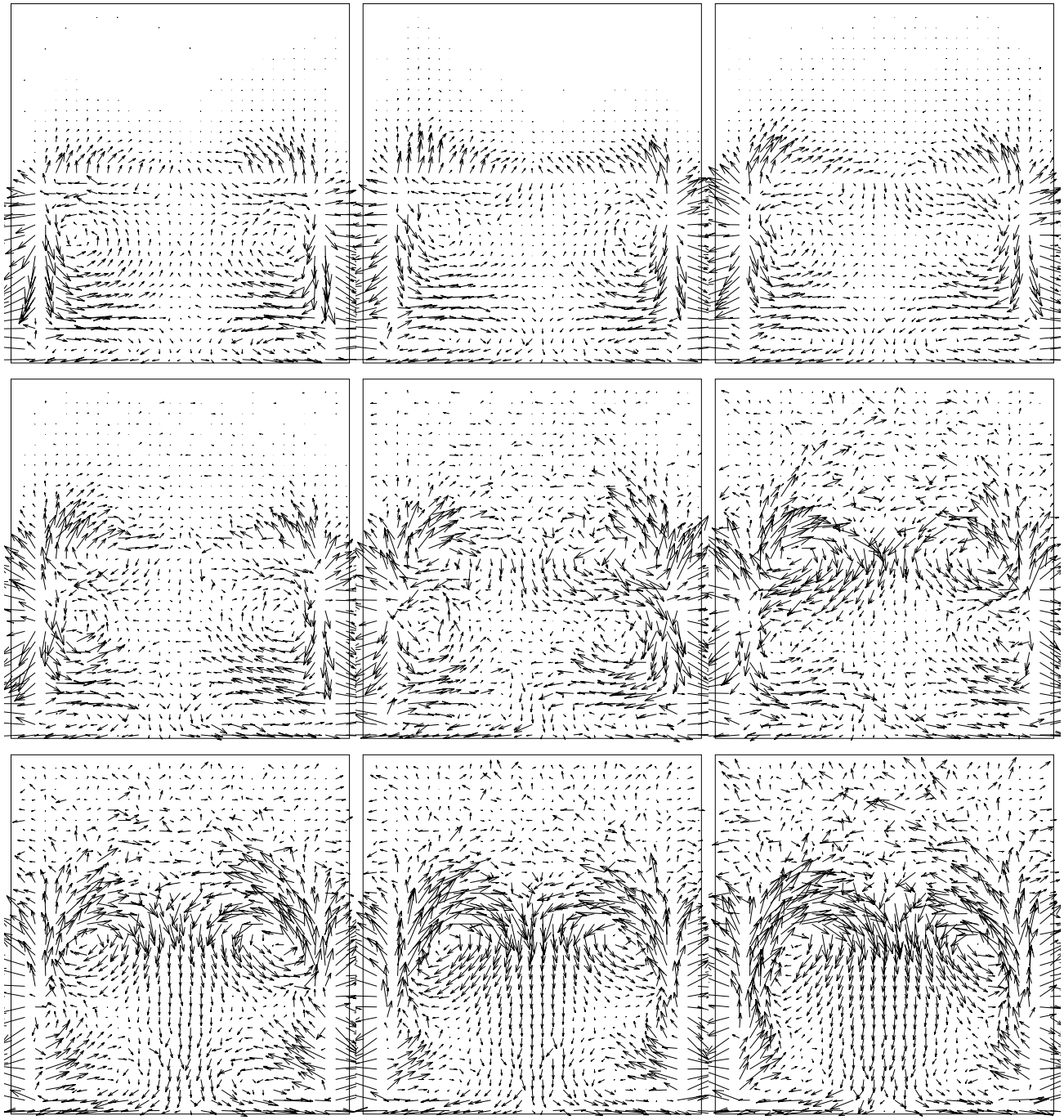

Fig. 2. Velocity field obtained after cycle averaging of particle displacements, for different values of the normal damping coefficient, γ_n. The first one is 1×10^4, and for obtaining each subsequent frame the coefficient has been divided by two. The frames are ordered from left to right and from top to bottom. The cell size for averaging is approximately one particle diameter.

of two surface rolls laying on top of the bulk cells and circulating in opposite direction. The second transition eliminates the bulk rolls.

A more detailed analysis of the displacement fields (Fig. 3) allows us to locate the transitions much more precisely. The horizontal axis shows the values of the normal damping coefficient γ_n scaled logarithmically in decreasing sequence. The vertical axis represents the position in vertical direction, with the free surface of the system located at $y \approx 60$. In Figure 3 we have represented in greyscale the horizontal and vertical components of the displacement vectors pictured in Figure 2 but in a denser sampling, analyzing data from 30 simulations corresponding to values of the normal damping coefficient within the interval [50, 10 000]. For horizontal displacements, we have chosen vertical sections at some representative position

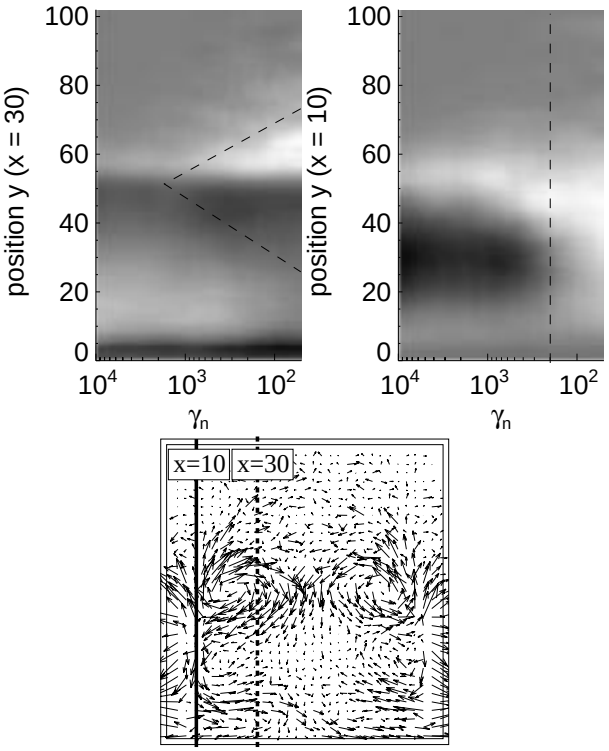

Fig. 3. Horizontal (left) and vertical (right) displacements at selected positions of the frames in Figure 2 (see the text for details), for decreasing normal damping γ_n and as a function of depth. White indicates strongest flow along positive axis directions (up, right), and black the corresponding negative ones. The black region at the bottom of the left picture corresponds to the complex boundary effect observed in Figure 2, involving only two particle layers. The figure below shows a typical convection pattern together with the sections at $x = 10$ and $x = 30$ at which the displacements were recorded.

in horizontal direction ($x = 30$). For the vertical displacements, vertical sections of the leftmost part of the container were selected ($x = 10$), see Figure 3, lower part.

One observes first that white surface shades, complemented by subsurface black ones, appear quite clearly at about $\gamma = 2000$ in Figure 3 (left), indicating the appearance of surface rolls. On the other hand, Figure 3 (right) shows a black area (indicative of downward flow along the vertical wall) that vanishes at $\gamma_n \approx 200$ (at this point the grey shade represents vanishing vertical velocity). The dashed lines in Figure 3 lead the eye to identify the transition values. In the interval $200 \lesssim \gamma_n \lesssim 2000$ surface and inner rolls coexist, rotating in opposite directions.

One can analyze the situation in terms of the restitution coefficient. From equation (1), the equation of motion for the displacement ξ_{ij} can be integrated and the relative energy loss in a collision $\eta = (E_0 - E)/E_0$ (with E and E_0 being the energy of the relative motion of the particles) can be evaluated approximately. Up to the lowest order in the expansion parameter, one finds [26]

$$\eta = 1.78 \left(\frac{\tau}{\ell} v_0\right)^{1/5}, \tag{5}$$

where v_0 is the relative initial velocity in normal direction, and τ, ℓ, time and length scales associated with the problem (see [26] for details),

$$\tau = \frac{3}{2}B, \quad \ell = \left(\frac{1}{3}\frac{m_{ij}^{\text{eff}}}{\sqrt{R_{ij}^{\text{eff}}}B\gamma_n}\right)^2. \tag{6}$$

For $\gamma_n = 10^4$ (the highest value analyzed) and the values of the parameters specified above ($v_0 \approx A2\pi f$ for collisions with the incoming wall), $B = 10^{-4}$ and η is typically 50%. This means that after three more collisions the particle leaves with an energy not enough to overcome the height of one single particle in the gravity field. For $\gamma_n = 10^3$ and the other parameters kept constant, $B = 10^{-5}$ and η has been reduced to 5%, resulting in that the number of collisions needed for the particle to have its kinetic energy reduced to the same residual fraction, has increased roughly by an order of magnitude. On the other hand, given the weak dependence of equation (5) on the velocity, one expects that the transitions shown in Figure 3 will depend also weakly on the amplitude of the shaking velocity. The reduction of the inelasticity η by an order of magnitude seems enough for particles to "climb" the walls and develop the characteristic surface rolls observed in numerical simulations.

4 Discussion

We have shown that the value of the normal damping coefficient influences the convective pattern of horizontally shaken granular materials. By means of molecular dynamics simulations in two dimensions we can reproduce the pattern observed in real experiments, which corresponds to a situation of comparatively high damping, characterized by inelasticity parameters η larger than 5%. For lower damping, the upper layers of the material develop additional surface rolls as has been reported previously. As normal damping decreases, the lower rolls descend and finally disappear completely at inelasticities of the order of 1%.

The authors want to thank R.P. Behringer, H.M. Jaeger, M. Medved, and D. Rosenkranz for providing experimental results prior to publication and V. Buchholtz, S.E. Esipov, and L. Schimansky-Geier for discussion. The calculations have been done on the parallel machine *KATJA* (http://summa.physik.hu-berlin.de/KATJA/) of the medical department *Charité* of the Humboldt University Berlin. The work was supported by Deutsche Forschungsgemeinschaft through grant Po. 472/3-2.

References

1. G. Strassburger, A. Betat, M.A. Scherer, I. Rehberg, in *Traffic and Granular Flow*, edited by D.E. Wolf, M.

Schreckenberg, A. Bachem (World Scientific, Singapore, 1996), p. 329.
2. G.H. Ristow, G. Strassburger, I. Rehberg, Phys. Rev. Lett. **79**, 833 (1997).
3. G.H. Ristow, Europhys. Lett. **40**, 625 (1997).
4. S.G.K. Tennakoon, L. Kondic, R.P. Behringer, Europhys. Lett. **45**, 470 (1999).
5. H.M. Jaeger, M. Medved (private communication, 1997).
6. D.E. Rosenkranz, T. Pöschel, `cond-mat/9712108` (1997); T. Pöschel, D. Rosenkranz, in *A Perspective Look at Nonlinear Media in Physics, Chemistry, and Biology*, edited by J. Parisi, S.C. Müller, W. Zimmermann (Springer, Berlin, 1998).
7. S.G.K. Tennakoon, R.P. Behringer, Phys. Rev. Lett. **81**, 794 (1998).
8. O. Pouliquen, M. Nicolas, P.D. Weidman, Phys. Rev. Lett. **79**, 3640 (1997).
9. K. Iwashita, Y. Tarumi, L. Casaverde, D. Uemura, K. Meguro, M. Hakuno, in *Micromechanics of Granular Material*, edited by M. Satake, J.T. Jenkins (Elsevier, Amsterdam, 1988), p. 125.
10. K. Liffman, G. Metcalfe, P. Cleary, Phys. Rev. Lett. **79**, 4574 (1997); K. Liffman, G. Metcalfe, in *Powders & Grains'97*, edited by R.P. Behringer, J.T. Jenkins (Balkema, Rotterdam, 1997), p. 405.
11. C. Salueña, S.E. Esipov, T. Pöschel, in *Powders & Grains'97*, edited by R.P. Behringer, J.T. Jenkins (Balkema, Rotterdam, 1997), p. 341; C. Salueña, S.E. Esipov, T. Pöschel, SPIE Proc. **3045**, 2 (1997); S.E. Esipov, C. Salueña, T. Pöschel (preprint, 1997).
12. C. Salueña, S.E. Esipov, T. Pöschel, S. Simonian, SPIE Proc. **3327**, 23 (1998); C. Salueña, T. Pöschel, S.E. Esipov, Phys. Rev. E **59**, 4422 (1999).
13. B. Drossel, T. Prellberg, Eur. Phys. J. B **1**, 533 (1998).
14. G. Rátkai, Powder Technol. **15**, 187 (1976); C. Laroche, A. Douady, A. Fauve, J. Phys. France **50**, 699 (1989).
15. H.M. Jaeger, S.R. Nagel, Science **255**, 1523 (1992); E.E. Ehrichs, H.M. Jaeger, G.S. Karczmar, J.B. Knight, V.Yu. Kuperman, S.R. Nagel, Science **267**, 1632 (1995).
16. M. Bourzutschky, J. Miller, Phys. Rev. Lett. **74**, 2216 (1995); H. Hayakawa, S. Yue, D.C. Hong, Phys. Rev. Lett. **75**, 2328 (1995).
17. J.A.C. Gallas, H.J. Herrmann, S. Sokołowski, Phys. Rev. Lett. **69**, 1371 (1992); Y. Taguchi, *ibid.*, 1367; J.A.C. Gallas, H.J. Herrmann, T. Pöschel, S. Sokołowski, J. Stat. Phys. **82**, 443 (1996); T. Pöschel, H.J. Herrmann, Europhys. Lett. **29**, 123 (1995).
18. In a certain range of parameters vertically shaken granular material may reveal complicated patterns as reported recently by C. Bizon, M.D. Shattuck, J.B. Swift, W.D. McCormick, H.L. Swinney, Phys. Rev. Lett. **80**, 57 (1998). Here, we refer to the simple large scale convective motion where material rises in the middle of the container and moves downwards close to the vertical walls.
19. For movies of horizontally shaken sand see `http://summa.physik.hu-berlin.de/~kies/Horizontal/`
20. P.A. Cundall, O.D.L. Strack, Géotechnique **29**, 47 (1979).
21. N.V. Brilliantov, F. Spahn, J.-M. Hertzsch, T. Pöschel, Phys. Rev. E **53**, 5382 (1996).
22. W.A.M. Morgado, I. Oppenheim, Phys. Rev. E **55**, 1940 (1997); Physica A **246**, 547 (1997); G. Kuwabara, K. Kono, Jpn J. Appl. Phys. **26**, 1230 (1987).
23. P.K. Haff, B.T. Werner, Powder Technol. **48**, 239 (1986).
24. Several authors describe the dissipation of colliding particles by a "coefficient of restitution" ϵ. Applying the correct normal force (1) for colliding non-cohesive particles [21,22] one finds that ϵ depends on their relative velocity [21,26]. Therefore, one cannot express γ_n in terms of ϵ.
25. M.P. Allen, D.J. Tildesley, *Computer Simulations of Liquids* (Clarendon Press, Oxford, 1987).
26. T. Schwager, T. Pöschel, Phys. Rev. E **57**, 650 (1998).